Development of Nanofiller-Modulated Polymeric Oxygen Enrichment Membranes for Reduction of Nitrogen Oxides in Coal Combustion

Dr. Jianzhong Lou (PI)
Dr. Shamsuddin Ilias (Co-PI)
Department of Mechanical and Chemical Engineering
North Carolina A&T State University
1601 E. Market St.
Greensboro, NC 27411
Phone: (336) 334-7620
FAX: (336) 334-7417
E-mail: lou@ncat.edu
Grant Number DE-FG26-06NT42742
Performance Period 2/17/06 – 2/16/09

OBJECTIVES

- (1) Develop a polymer material that incorporates functional nanofillers to achieve novel oxygen-enrichment permselectivity;

- (2) Document the fundamental microstructure-property relationship of the nanofiller-modulated polymer material using molecular simulation.

Gas-Separation Membrane Parameters

Mass transfer flux $J_A = P_A\left(\frac{dp_A}{dx}\right) = D_A\left(\frac{dc_A}{dx}\right)$

p_A partial pressure of gas molecule A

c_A concentration of gas molecule A

P_A Permeability of polymer for gas molecule A

D_A Difusion coefficient of gas molecule A inside polymer

$$S_A = \frac{c_A}{p_A}$$

S_A Solubility of gas molecule A inside polymer

Separation factor (also called selectivity) $\alpha_{A/B} = \frac{P_A}{P_B}$

Measurement of Diffusion Coefficient

$$D = \frac{\ell^2}{6\theta} \qquad (12.22)$$

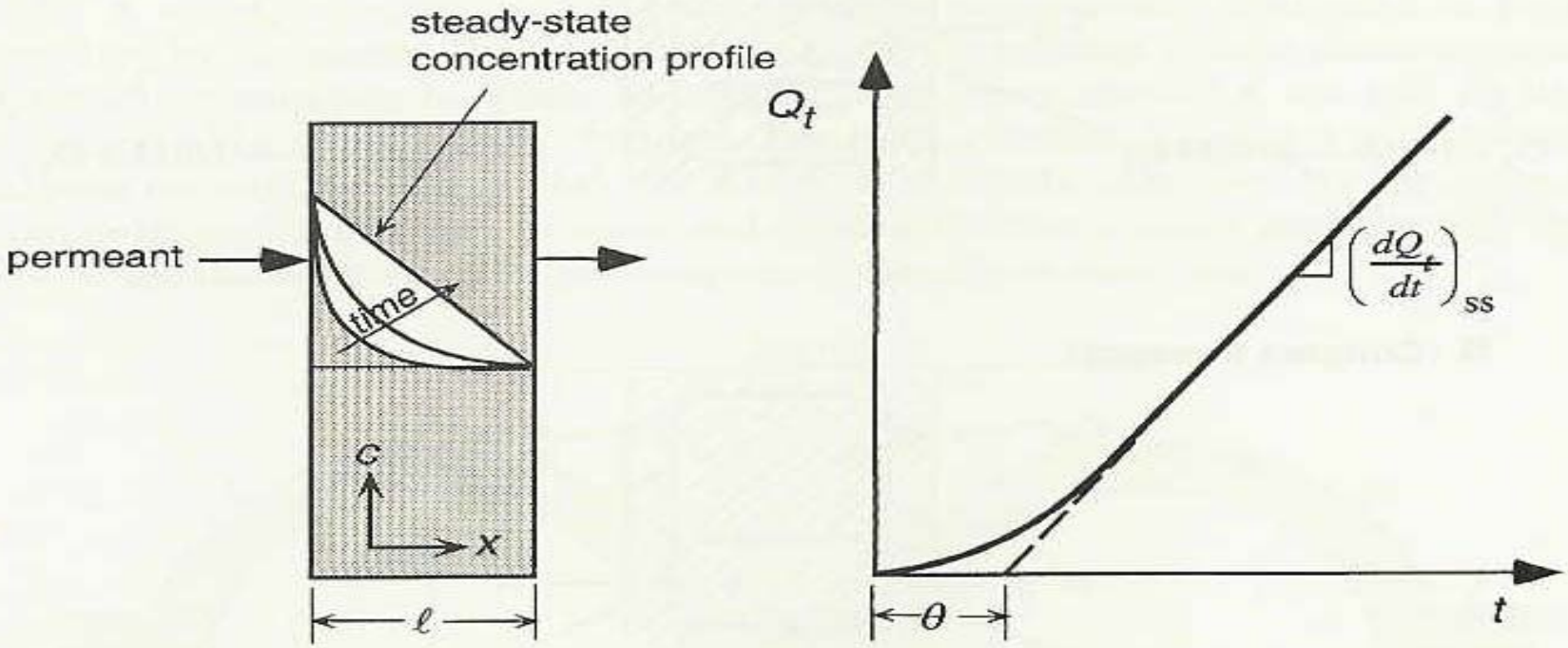

Figure 12-10 Plot of the amount of permeant versus time for a flat film illustrated at the left. The slope of the linear portion of the curve gives the steady-state permeability, while the intercept with the time axis yields the time lag, θ, from which the apparent diffusion coefficient can be obtained (eq. 12.22). The increase in permeant concentration in the film up to the attainment of steady state is illustrated at the left.

Measurement of Solubility

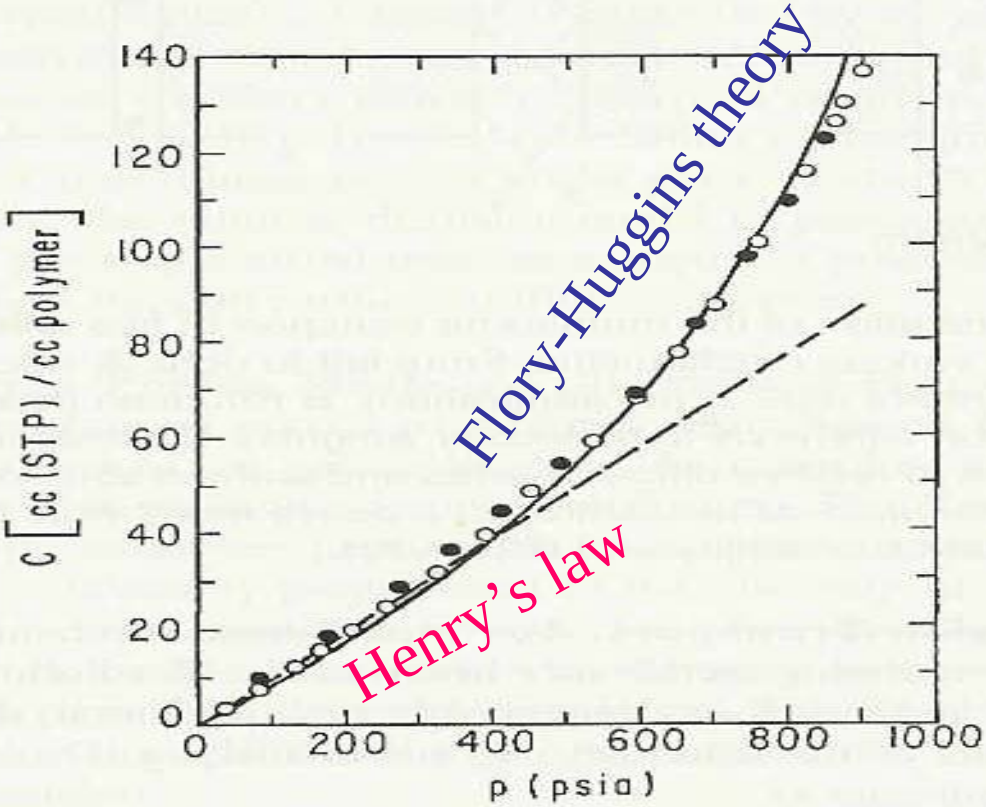

Figure 12-8 Sorption isotherm of CO_2 in silicone rubber at 35°C. Data points give CO_2 concentrations measured at different pressures during sorption (○) and desorption (●). The solid line represents the fit by the Flory–Huggins equation; the broken line represents Henry's law behavior. (Reprinted with permission from G. K. Fleming and W. J. Koros, *Macromolecules*, **19**, 2285 (1986). Copyright 1986 American Chemical Society.)

Table 12-7 Kinetic Diameters and Lennard-Jones Potential Well Depth* of Important Gases

Gas:	He	H_2	CO_2	O_2	N_2	CO	CH_4
Kinetic diameter (Å)	2.6	2.89	3.3	3.46	3.64	3.76	3.80
ε/k (K)	10.2	59.7	195	107	71.4	91.7	149
σ (Å)	2.55	2.83	3.94	3.47	3.80	3.69	3.76

*See text footnote for identification of the Lennard-Jones ε/k and σ parameters.

Table 12-5 Gas Permeability and Permselectivity of Representative Polymer (at 25° to 35°C)

Polymer	$P(O_2)^*$	$\frac{P(O_2)}{P(N_2)}$	$P(CO_2)$	$\frac{P(CO_2)}{P(CH_4)}$
Rubbery Polymers				
High-density polyethylene ($\rho = 0.964$)	0.4	2.9	1.7	4.4
Butyl rubber	1.3	3.9	5.8	6.6
Low-density polyethylene ($\rho = 0.914$)	2.9	3.0	12.6	4.3
Natural rubber	24	3.0	134	4.7
Silicone rubber	610	2.2	4,553	3.4
Glassy Polymers				
Poly(ethylene terephthalate) ($X_c = 0.50$)	0.06	4.5	0.30	—
Cellulose acetate	0.68	3.4	5.5	28
Polysulfone	1.3	5.2	4.9	23
Polycarbonate	1.5	5.2	6.0	23
Polystyrene	2.6	3.3	10.5	—
Poly(2,6-dimethyl-1,4-phenylene oxide)	18	5.0	59	15
Poly(4-methylpentene-1)	29	4.4	93	—
Poly[1-(trimethylsilyl)-1-propyne]	7,200	1.7	19,000	4.4

* Permeability in barrers [10^{-10} cm^3 (STP)-cm/(cm^2-s-cm Hg)]

Polydimethylsiloxane membrane

Table 12-1 Permeability Coefficients of Selected Polymers at 25°C*

Polymer	$P(O_2)^{\dagger}$
Poly(vinyl alcohol)	~0.0001
Polyacrylonitrile	~0.002
Poly(vinylidene chloride)	0.012
Polymethacrylonitrile	0.012
Poly(ethylene terephthalate)	0.42
Poly(vinyl chloride)	0.48
Poly(vinyl acetate)	3.3
Polypropylene	10.8
Polyethylene (LDPE)	30.0
Polyisobutylene	90.0
Polydimethylsiloxane	~3000

*Data taken from ref. 1.

$^{\dagger}P \times 10^{11}$ cm^3-cm/cm^2-sec cmHg at 0% humidity

$^{\ddagger}P \times 10^{11}$ g-cm/cm^2 sec cmHg

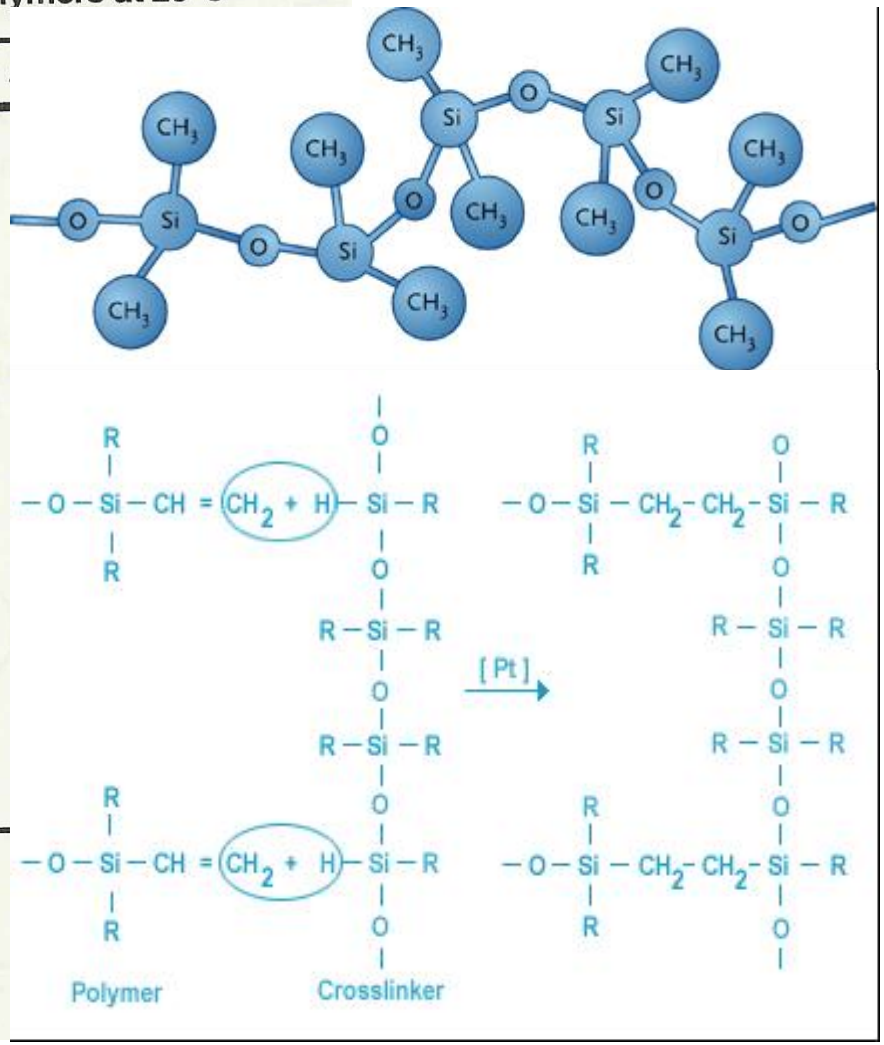

Polyimide membrane

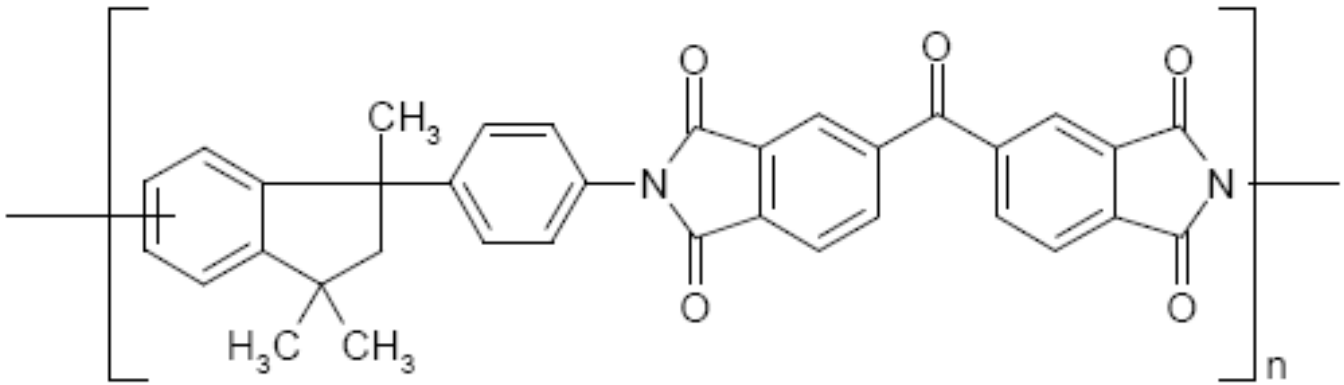

- Huntsman Matrimid 5218
- Fully imidized
- Soluble in a variety of organic solvents
- Tg = 280 ^{o}C

Membrane preparation

- Preferred method for application of thin, uniform films to flat substrates.
- The polymer solution placed on the substrate is rotated at high speed in order to spread the fluid by centrifugal force.
- Rotation is continued for some time, with fluid being spun off the edges of the substrate, until the desired film thickness is achieved.

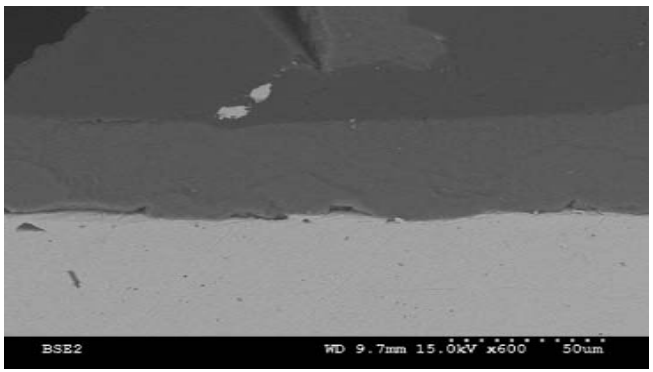

Neat polymer 18 μm thick

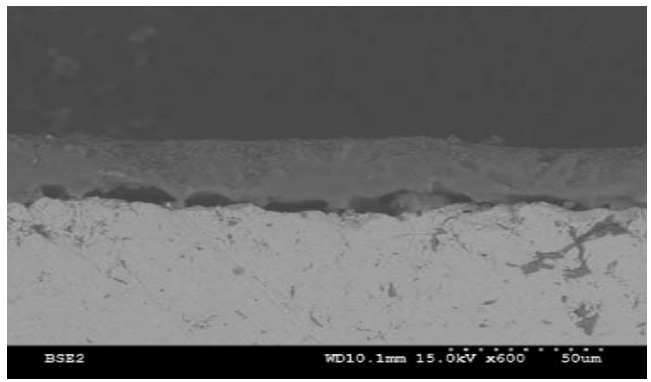

Filled polymer 28 μm thick

Membrane permeation test

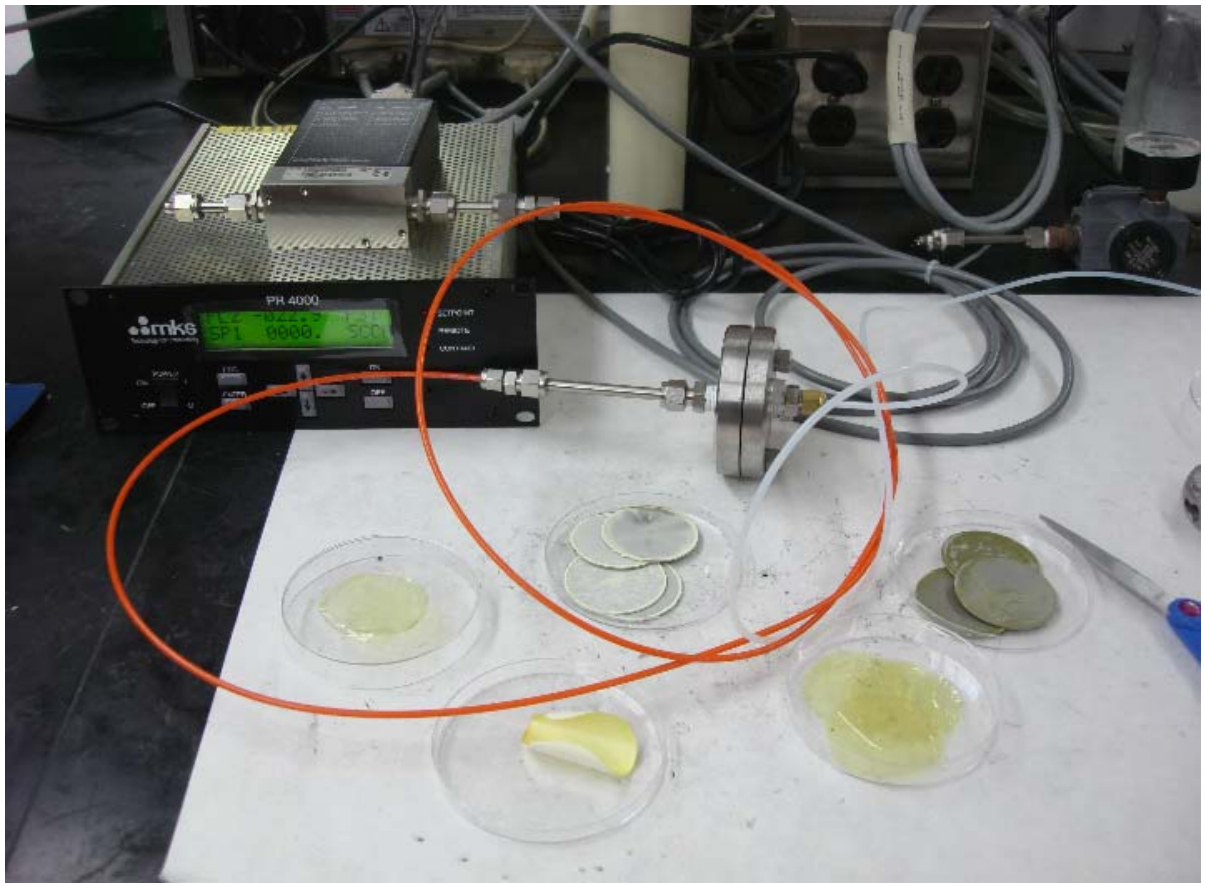

Polymer Characterization

PDMS-Carbon Nanotube Membrane

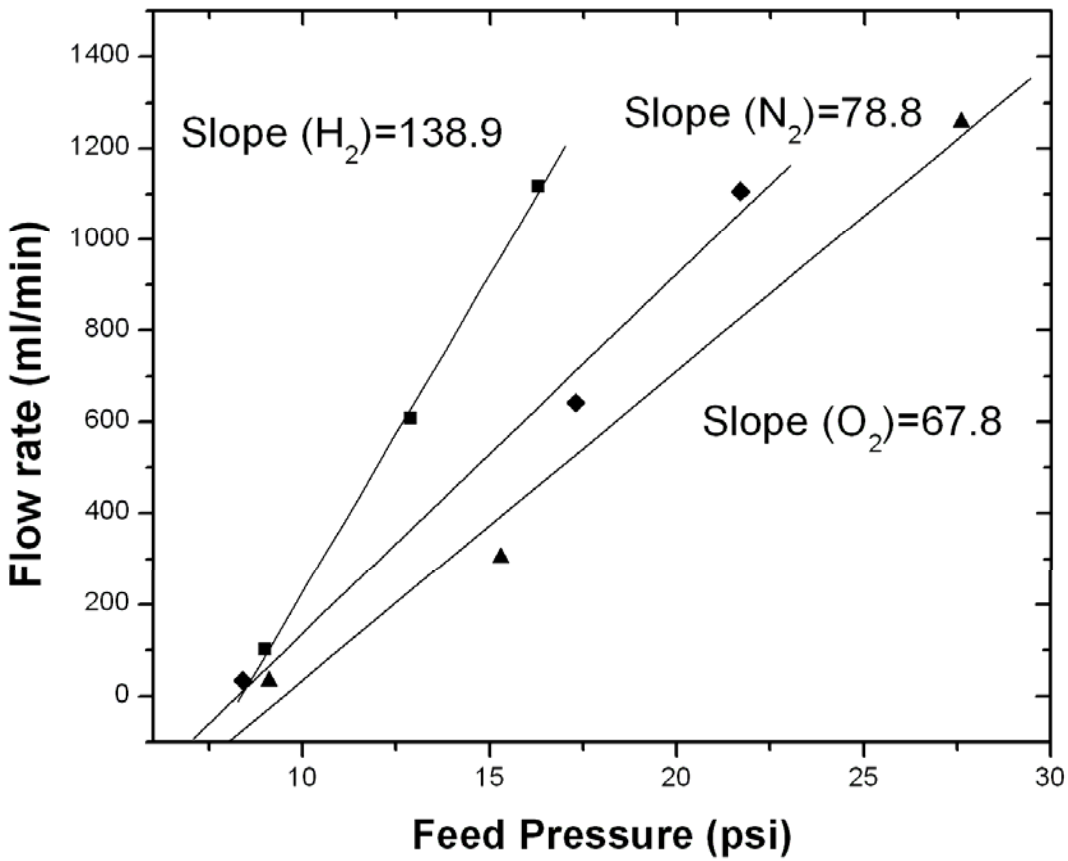

Selectivity	Neat PDMS	PDMS+MWNT
Oxygen/Nitrogen	1.97	0.86
Hydrogen/Oxygen	1.01	2.05

PDMS-Silica Membrane

Neat PDMS

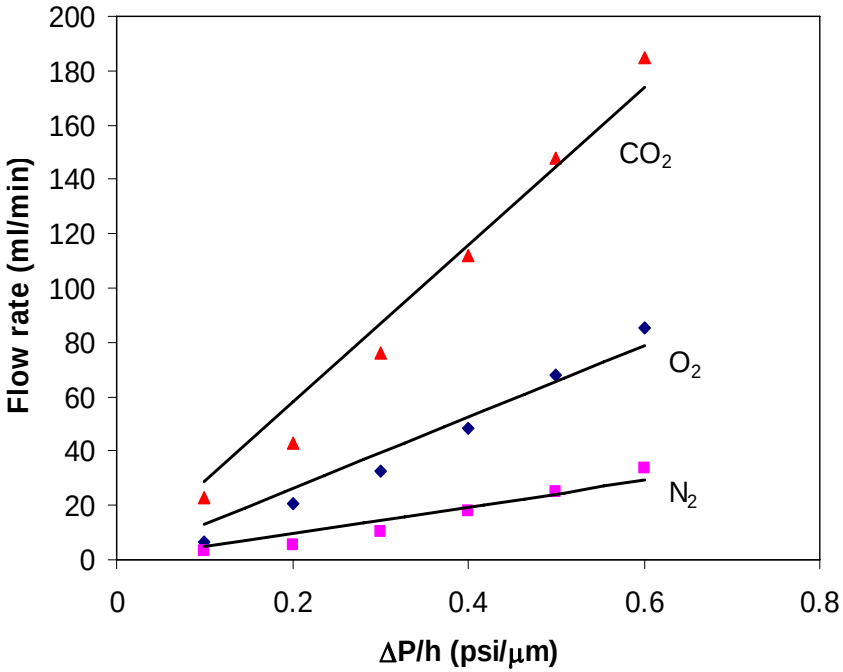

Filled PDMS

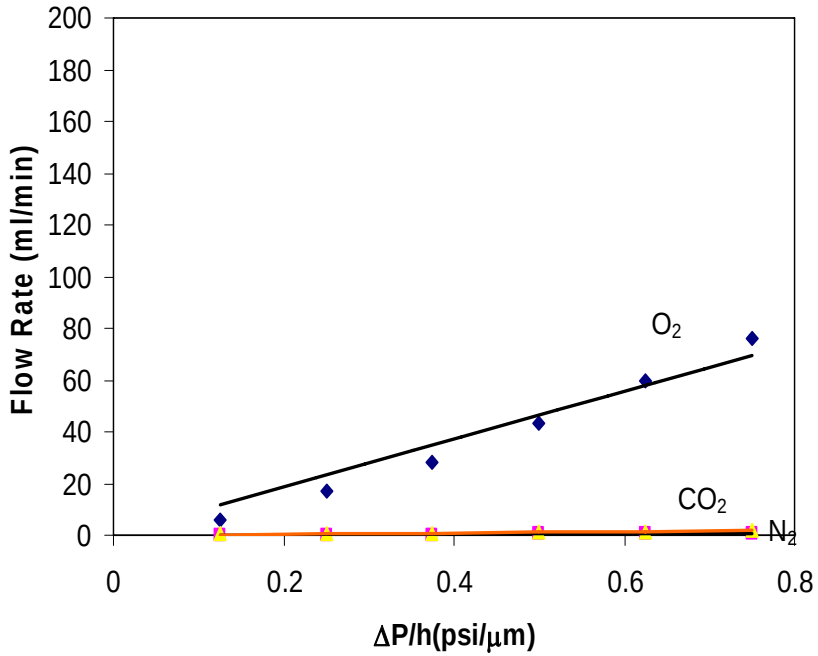

$$J_A = P_A\left(\frac{dp_A}{dx}\right) = D_A\left(\frac{dc_A}{dx}\right)$$

$$\alpha_{Oxygen\ /\ Nitrogen} = \frac{P_{O2}}{P_{N2}} = \frac{J_{O2}\cdot p_{N2}}{J_{N2}\cdot p_{O2}}$$

Diffusion Coefficient

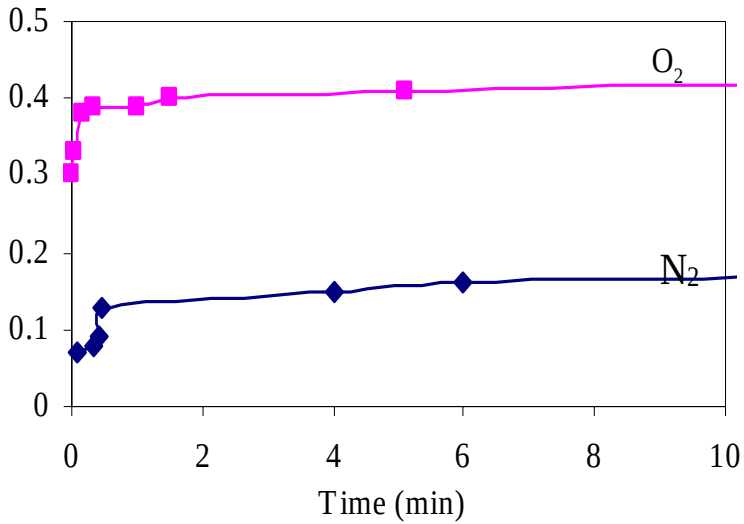

Response of permeate pressure for neat PDMS- time lag method

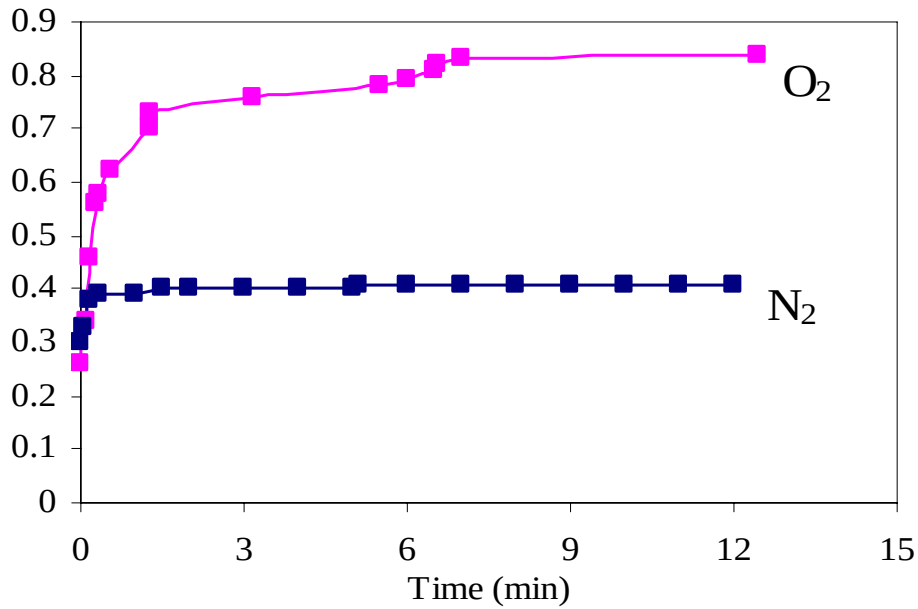

Response of permeate pressure for filled PDMS- time lag method

Selectivity of O_2/N_2	PDMS	Filled PDMS
$\alpha_{A/B}$	2.04	8.54

Polymer-Carbon Nanotube Membrane

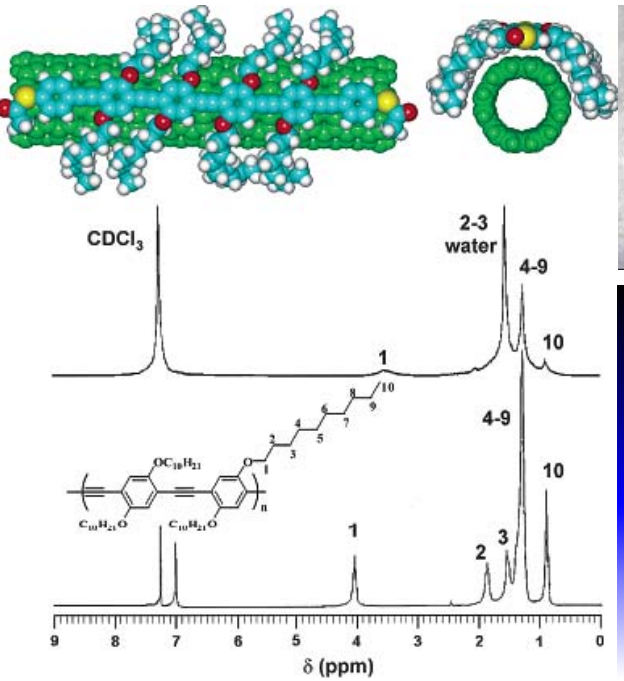

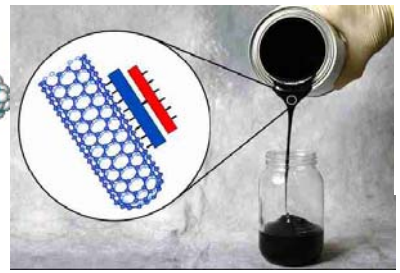

zyvex®
www.zyvex.com

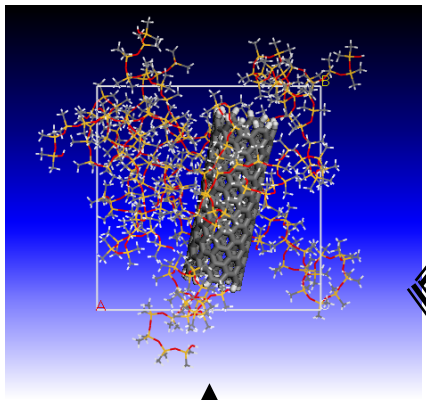

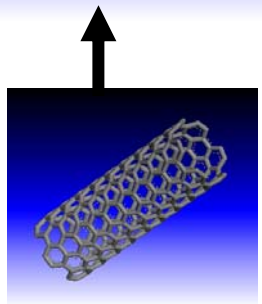

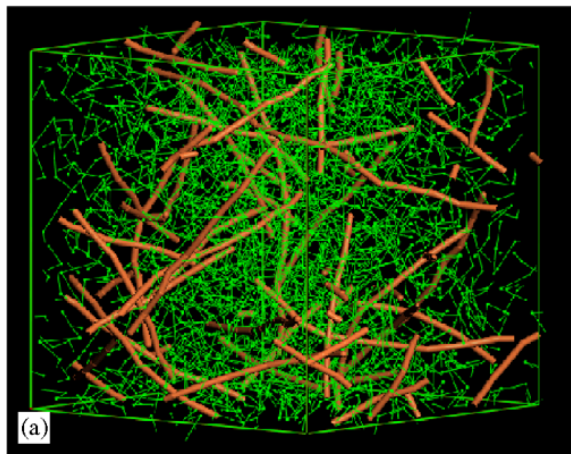

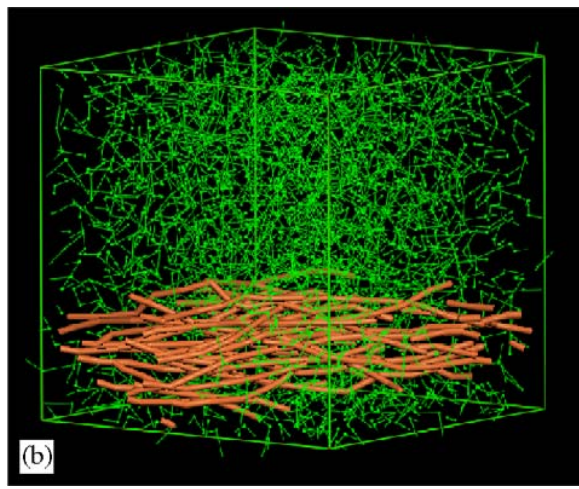

A molecular model of **1a***n*)1.5-SWNT(6,6) complex (top) and 1H NMR spectra (300 MHz, CDCl3) of **1a** (bottom) and **a**-SWNTsHiPco complex (middle). [Jian Chen etc. *J.Am. Chem. Soc.* **2002**, *124*, 9034-9035]

Molecular Modeling and Simulations

Nanofiller

Nanocomposite

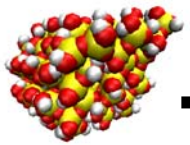

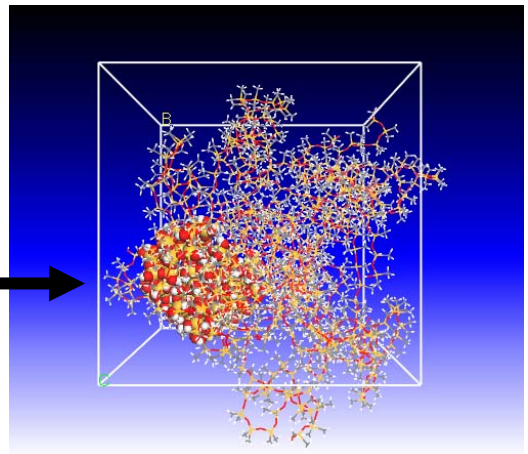

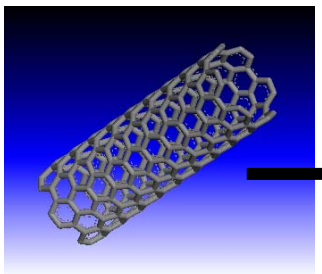

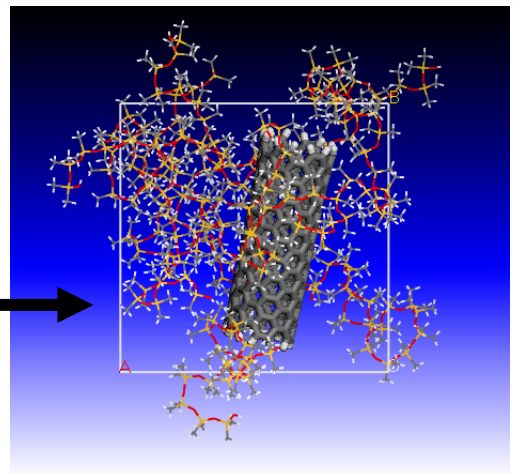

Modified GROMOS force field

Bonds	k_b (10^5/kJ mol^{-1} nm^{-2})	b_0 (nm)
Si–O	2.5080	0.160
Si–CH_3	2.5080	0.188
Angles	k_Θ (kJ/mol^{-1} rad^{-2})	Θ_0 (deg)
Si–O–Si	118.4	114.0
O–Si–O	791.2	109.5
O–Si–CH_3	418.4	109.5
CH_3–Si–CH_3	418.4	109.5
Dihedrals	k_φ (kJ mol^{-1})	n δ
CH_3–Si–O–Si	3.77	3 0
Si–O–Si–CH_3	3.77	3 0
Si–O–Si–O	3.77	3 0
O–Si–O–Si	3.77	3 0

Nonbonded	ϵ (kJ mol^{-1})	σ (nm)	$q(e)$	(a.m.u)
Si	2.4480	0.3385	0.3	28.080
O	0.8493	0.2955	−0.3	15.999
CH_3 (PDMS)	0.7532	0.3786	0	15.035
He	0.0850	0.2580	0	4.003
H_2	0.3076	0.2950	0	2.016
Ar	0.9977	0.3400	0	39.948
N_2	0.7898	0.3700	0	28.013
O_2	0.9145	0.3500	0	31.998
CH_4	1.2466	0.3733	0	16.043

Potential energy

- The potential energy of the chosen simulation system was calculated using the GROMACS implementation of the modified OPLS-AA force field

$$E_{PE} = \sum_{bonds} k_r \left(r - r_0\right)^2 + \sum_{angles} k_\theta \left(\theta - \theta_0\right)^2 + \sum_{impropers} k_\xi \left(\xi - \xi_0\right)^2$$

$$+ \sum_{n=0}^{5} C_n \left(\cos(\Psi)\right)^n + \sum_i \sum_{j>i} f_{ij} \left\{ \frac{q_i q_j e^2}{r_{ij}} + 4\varepsilon_{ij} \left[\left(\frac{\sigma_{ij}}{r_{ij}} \right)^{12} - \left(\frac{\sigma_{ij}}{r_{ij}} \right)^{6} \right] \right\}$$

The nontorsional bonded interactions are modeled by first three harmonic terms for bond stretching, angle bending, and out of plane deformations for planar groups. The force constants for intramolecular deformations $\left(k_r, k_\theta, k_\xi\right)$ define the magnitude of the energy required to move the internal coordinates $\left(r, \theta, \xi\right)$ away from their unstrained default values $\left(r_0, \theta_0, \xi_0\right)$. The proper torsions are defined in terms of the specific dihedral angle (Ψ) and Ryckaert-Bellemans potential parameter C_n, where n = 0, 1… 5. The nonbonded interactions are modeled by Coulombic and 6-12 Lennard-Jones terms, where r_{ij} is the distance of two sites, q is the partial atomic charge, and and are the Lennard-Jones parameters. The scaling factor is 1.0 for all nonbonded interactions except for the 1, 4-intramolecular interactions.

Prediction of diffusion coefficient

- To determine the self diffusion coefficient D_N, one can use the Einstein relation.
- The terms in the angular brackets represent the time averaged mean-square displacement (MSD). After approximately 100ps, the molecules will be moving in a totally random fashion (Brownian motion), and the mean-square deviation of the system will increase linearly as the atoms drift away from each other. The MSD from 200ps to 800ps was fit to a linear curve and the slope is directly related to the self diffusion coefficient.

$$\lim_{t\to\infty}\left\langle \left\| r_i(t) - r_i(0) \right\|^2 \right\rangle_{t\in N} = 6D_N t$$

MD simulations

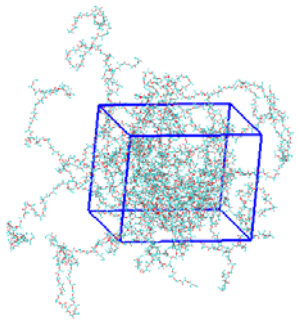

Polymer matrix box

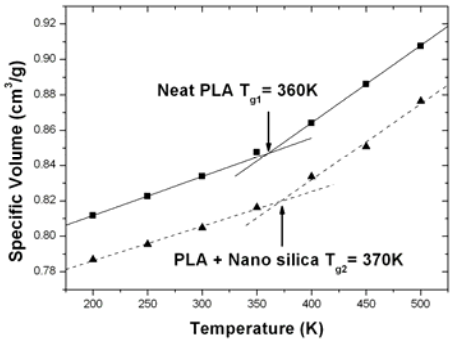

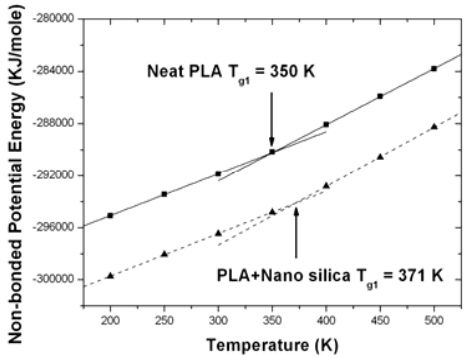

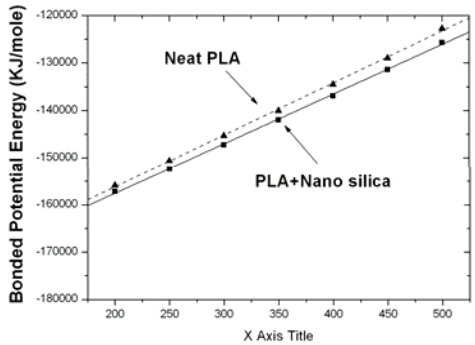

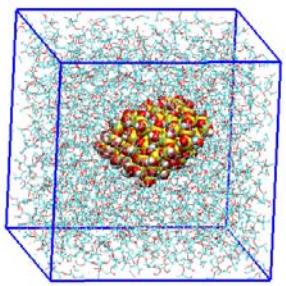

Nanosilica box partical diameter is about 2 nm

MD Simulations vs Experiments

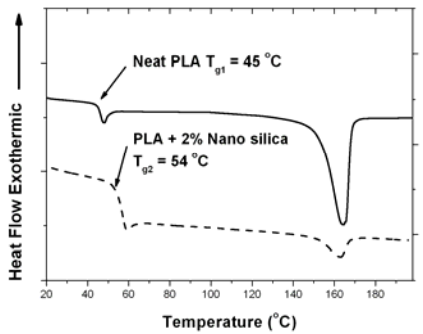

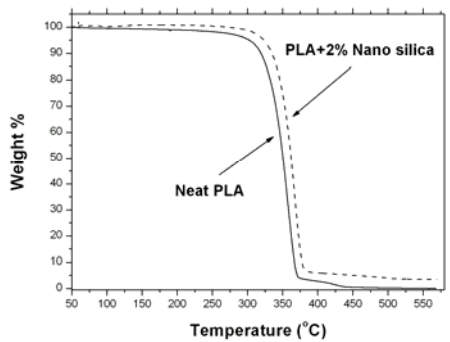

Diffusion Coefficient

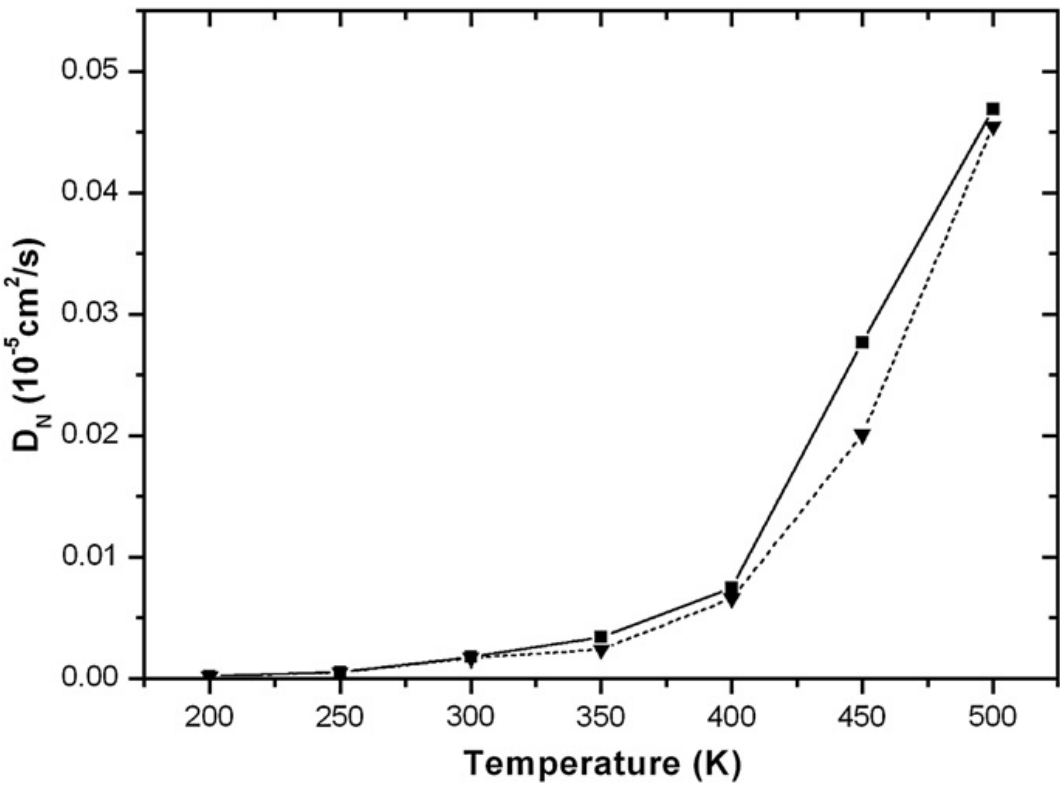

Predicted self-diffusion coefficient D as a function of temperature for neat polymer and nanocomposite chains around silica nanoparticles (bottom).

Results Summary

- The influence of nanofillers on the self diffusion, free volume, glass transition and in turn the oxygen diffusion and solubility and the permselectivity of oxygen in polymer membrane is studied.
- Thermal properties were investigated by experiments and molecular dynamics simulations. Molecular models of Single-walled carbon nanotubes PDMS membrane and nano fumed silica PDMS membrane, zeolite-modulated polyimide membrane were built by Material Studio 4.0 and the resulting output coordinate files were modified to make them compatible with GROMACS.
- All Molecular dynamics simulations were performed using the GROMACS 3.3 simulation package on a 40-node IBM xSeries Linux Cluster. Modified OPLS-AA force field was used. In the simulations, the leapfrog algorithm was used to integrate Newton's equations of motion with a time step of 2 fs. Periodic boundary conditions were applied and nonbonded force calculations employed a grid system for neighbor searching. In this system, only the atoms in the neighboring grid cells are considered when building a new neighbor list. A twin-range cutoff was used for both Lennard-Jones and Coulombic calculations.
- The permeation and diffusion experiments were performed for the different membranes with different amount of nanofillers.

LIST OF PAPERS/PATENT PUBLISHED

- 1. J. Zhang, **J. Lou**, S. Ilias, P. Krishnamachari, J. Yan. “Thermal properties of poly(lactic acid) fumed silica nanocomposites: Experiments and molecular dynamics simulations”, Polymer, **2008** 49, 2381-2386.

- 2. J. Zhang, Y. Liang, J. Yan, **J. Lou**, “Study of molecular weight dependence of glass transition temperature for amorphous poly(l-lactide) by molecular dynamics simulation”, Polymer. **2007** 48, 4900-4905.

- 3. **J. Lou**, V. Harinath, S. Ilias, J. Sankar, “An ultrahigh-selectivity oxygen enrichment filled elastomeric silicone polymer membrane incorporating nanofillers”, U.S. 7,264,650, **2007**.

Acknowledgement

- Mr. Timthy Fout, NETL Project Manager
- NETL Grant DE-FG26-06NT42742

References

- [1] T. C. Merkel; Freeman, B. D.; Spontak, R. J.; He, Z.; Pinnau, I.; Meakin, P.; Hill, A. J., "Sorption, transport, and structural evidence for enhanced free volume in poly(4-methyl-2-pentyne)/fumed silica nanocomposite membranes", Chemistry of Materials, 15(1), 109-123 (2003).

- [2] N. F. A. van der Vegt, W. J. Briels, M. Wessling, and H. Strathmann, "Free energy calculations of small molecules in dense amorphous polymers. Effect of the initial guess configuration in molecular dynamics studies," J. Chem. Phys. 1996 (105). pp. 8849-8857

- [3] Jian Chen etc. *J.Am. Chem. Soc.* 2002, *124*, 9034-9035

- [4] Ho Bum Park, Chul Ho Jung, Young Moo Lee, Anita J. Hill, Steven J. Pas, Stephen T. Mudie, Elizabeth Van Wagner, Benny D. Freeman, David J. Cookson, "Polymers with Cavities Tuned for Fast Selective Transport of Small Molecules and Ions", Science, 2007, 318, 254-258